Separation Science and Technology
Publication details, including instructions for authors and subscription information:
http://www.informaworld.com/smpp/title~content=t713708471

A Macrokinetic Modeling of Membrane Microfiltration Processes

Michio Nonaka[a]
[a] DEPARTMENT OF MINERAL DEVELOPMENT ENGINEERING, THE UNIVERSITY OF TOKYO, TOKYO, JAPAN

To cite this Article Nonaka, Michio(1988) 'A Macrokinetic Modeling of Membrane Microfiltration Processes', Separation Science and Technology, 23: 4, 387 — 411
To link to this Article: DOI: 10.1080/01496398808060712
URL: http://dx.doi.org/10.1080/01496398808060712

SEPARATION SCIENCE AND TECHNOLOGY, 23(4 & 5), pp. 387-411, 1988

A Macrokinetic Modeling of Membrane Microfiltration Processes

MICHIO NONAKA

DEPARTMENT OF MINERAL DEVELOPMENT ENGINEERING
THE UNIVERSITY OF TOKYO
TOKYO 113, JAPAN

Abstract

Membrane microfiltration techniques have been developed and utilized mostly in the fields of gas purification and aerosol filtration. They were recently applied to medical, pharmaceutical, liquor, and food processings. Membrane microfiltration behavior is characterized by intrapore diffusive deposition of fine particles, surface pore blocking, and the formation of a thin cake layer on the filter surface. The intrapore diffusive deposition process predominates and it can be regarded macroscopically as a first-order rate process. The surface pore blocking process is also described by a first-order rate equation. Thus the filtration characteristics, such as filtration rate and filtration resistance, can be evaluated by using the macrokinetic models derived from first-order rate equations. The microfiltration processes were simulated numerically by these models and the calculation results agreed well with experimental observations. The backflushing stages must be included in a practical microfiltration process. A first-order rate process was proposed for the detachment process of collected particles from filter pores. Membrane microfiltration systems with backflushing stages were also evaluated macrokinetically and the effect of backflushing on the filtration performance was manifested numerically.

INTRODUCTION

Membrane microfiltration techniques have been developed and utilized mostly in the fields of gas purification and aerosol filtration. They have recently played an important part in medical, pharmaceutical, liquor, and food processings. In wastewater treatment systems, membrane microfiltration should contribute to developing more advanced

treatment processes, i.e., microfiltration stages can be incorporated in a treatment system to replace a part of conventional deep bed filtration processes. The methodology can also be applied to water supply processes in which the smallest colloidal particles, which are difficult to collect, have to be removed.

The mechanism of membrane microfiltration has been analyzed by using Pich's capillary model (*1*) and the Navier-Stokes equation to describe the flow in and around a filter pore (*2–5*). These approaches are, however, too complicated to evaluate such filtration performances as filtration rate, filtration resistance, and turbidity of the filtrate, which are essential factors for determining the optimum operating conditions involved in a membrane microfiltration process.

Membrane microfiltration behaviors are characterized mainly by intrapore and surface diffusive deposition of fine particles, surface pore blocking, and the formation of a thin cake layer on the filter surface. In this paper the diffusive deposition on the filter surface is disregarded and the intrapore diffusive deposition process or the surface pore blocking process is regarded as a first-order rate process. Then macrokinetic models are proposed to evaluate the filtration performances in terms of the operating variables. These kinetic models are verified successfully through a series of membrane microfiltration tests. Finally, the characteristics of membrane microfiltration systems with backflushing stages are evaluated from kinetic viewpoints.

INTRAPORE DIFFUSIVE DEPOSITION

In membrane microfiltration for a solid–liquid system containing particles finer than the filter pore size, solid particles are first collected by diffusive deposition on the inner pore walls and the filter surface. Assuming that the intrapore diffusive deposition is predominant and the surface diffusive deposition can be disregarded, the microfiltration process is formulated by taking into account the radial diffusion of particles and the flow velocity in a filter pore. Disregarding the axial diffusion of particles and the radial advection of the fluid, the diffusion process for monodispersed particles in a cylindrical filter pore is described by

$$\frac{\partial N}{\partial \tau} = \frac{\partial^2 N}{\partial x^2} + \frac{1}{x}\frac{\partial N}{\partial x} - \frac{\mathrm{Pe}}{2} U \frac{\partial N}{\partial y} \tag{1}$$

in the cylindrical coordinate system. The dimensionless terms are defined by

$$\left.\begin{array}{lll} C/C_0 = N; & Dt/R^2 = \tau; & r/R = x \\ z/R = y; & u_z/u_0 = U; & 2Ru_0/D = \mathrm{Pe} \end{array}\right\} \tag{2}$$

where r and z denote radial and axial coordinates, respectively, C and C_0 are concentrations at time t and $t = 0$, respectively, R is the pore radius, D is the diffusion coefficient, and u_z and u_0 are axial flow velocities at r and $r = 0$, respectively. Hence, the diffusive deposition process is written

$$\frac{\partial^2 N}{\partial x^2} + \frac{1}{x}\frac{\partial N}{\partial x} - \frac{\mathrm{Pe}}{2} U \frac{\partial N}{\partial y} = 0 \tag{3}$$

in the steady state. The boundary conditions are given by

$$\left.\begin{array}{rl} x = 0; & \partial N/\partial x = 0 \\ y = 0; & N = 1 \\ x = 1 - (a/R); & N = 0 \end{array}\right\} \tag{4}$$

Equation (3) was solved numerically by using the modified Saul'yev scheme (*6*) by assuming that the radial distribution of the axial velocity of the fluid in a pore is uniform or fully developed. The distributions of the normalized concentrations of nondeposited particles in the axial direction are shown in Fig. 1. As can be seen, the profile of the axial fluid velocity does not significantly affect the deposition behavior of particles when the Peclet number is not as large as expected in practical operation. Furthermore, it is confirmed that the relationship between y and N is formulated approximately by an exponential function. Then, by replacing directly the transport length of particles in a pore with the transport time, the diffusive deposition process is written as a first-order rate process. In the polydispersed system the intrapore diffusive deposition process is described as a combined form of the respective first-order rate process for nearly monodispersed particles involved in each size fraction.

MACROKINETIC MODEL

The intrapore diffusive deposition process for monodispersed particles is written macorkinetically as

$$-dC/dt = k_D C \tag{5}$$

where k_D is the diffusive deposition rate constant and hence

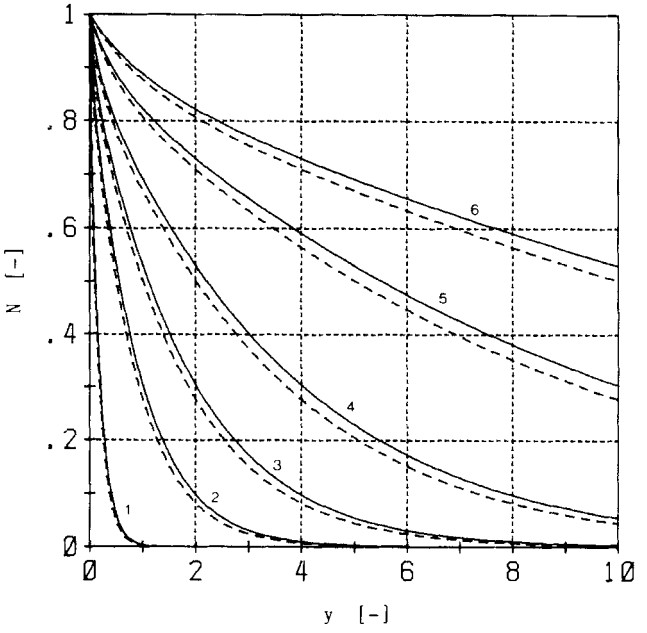

FIG. 1. Diffusive deposition of monodispersed particles on the inner wall of a filter pore. $a/R = 0.5$. $D = 10^{-11}$ m^2/s. (——) Uniform flow. (— —) Fully developed flow. Pe = 10 (1), 50 (2), 100 (3), 200 (4), 500 (5), 1000 (6).

$$C = C_0 \exp(-k_D t) \tag{6}$$

is obtained. Equation (6) is modified to

$$C = C_0 \int_0^\infty \delta(t) \exp(-k_D t) dt$$

$$= C_0 \exp(-k_D \theta) \tag{7}$$

is a continuous system under plug flow condition in a filter pore, where $\delta(t)$ denotes Dirac's delta function and θ is the mean residence time of particles through the pore. The filter pore is recognized as a macrospace composed of many minute plug flow regions connected in series. Hence, θ in Eq. (7) can be redefined as continuous time and rewritten as t.

The effective volume of a filter pore is reduced as particles are diffusively deposited on the pore wall. The volume at time t will be

$$\pi[R^2L - \tfrac{4}{3}a^3VC_0\{1 - \exp(-k_Dt)\}]$$

where L is the pore length, a is the particle radius, and V is the total flow volume. Assuming that the pore keeps the cylindrical configuration even when particles are deposited, the effective pore radius is written as

$$R_D = \left[R^2 - \frac{4}{3}\frac{a^3}{L}VC_0\{1 - \exp(-k_Dt)\}\right]^{1/2} \tag{8}$$

Hence, the volume flow rate through a pore under constant pressure is given by

$$\left(\frac{dV}{dt}\right)_D = \left(\frac{dV}{dt}\right)_{D,0}\left(\frac{R_D}{R}\right)^4 \tag{9}$$

where the subscripts D and 0 mean diffusion controlling and initial state, respectively. Equation (9) also represents the filtration rate per unit filter area in the diffusive rate-determining period.

The filtration characteristics of polydispersed particles can also be evaluated macrokinetically in a similar manner. Thus, assuming that particles are distributed discretely in size and there are no interactions between them, the effective pore radius is given by

$$R_D = \left[R^2 - \frac{4V}{3L}\sum a_i^3C_{0,i}\{1 - \exp(-k_{D,i}t)\}\right]^{1/2} \tag{10}$$

where the subscript i means the ith class of particle size. Hence, the filtration rate is derived by substituting Eq. (10) for R_D involved in Eq. (9). Moreover, it is reasonable that the first-order rate constant is distributed even in the monodispersed system due to the heterogeneity of the inner pore structure of the filter medium, the shape, and the surface properties of particles. Thus Eq. (8) has to be written as

$$R_D = \left[R^2 - \frac{4V}{3L}a^3C_0\left\{1 - \sum w_j \exp(-k_{D,j}t)\right\}\right]^{1/2} \tag{11}$$

when the rate constant is distributed discretely, where $k_{D,j}$ is the jth component of the distributed rate constants and w_j is the spectrum density. Consequently, the filtration rate is derived by substituting Eq. (11) for R_D involved in Eq. (9).

The membrane microfiltration process in the solid–liquid system

containing larger particles than the filter pore can be evaluated by taking into account the surface pore-blocking mechanism. Then it is assumed that the pore-blocking process is described by a first-order rate equation written as

$$-dM/dt = k_B M \tag{12}$$

where M denotes the number of open pores per unit filter area remaining unblocked at time t, and k_B is the blocking rate constant varied with the concentration of larger particles than the pore size. Hence, putting $M = M_0$ at $t = 0$,

$$M = M_0 \exp(-k_B t) \tag{13}$$

is derived. The volume flow rate per filter area is varied proportionately with the number of unblocked pores and, hence, it is given by

$$\left(\frac{dV}{dt}\right)_B = \left(\frac{dV}{dt}\right)_{B,0} \exp(-k_B t) \tag{14}$$

where the subscript B means surface blocking controlling. The increase of the filtration resistance per unit volume of the filtrate is derived from Eq. (14) and represented as

$$\frac{d}{dV}\left(\frac{dt}{dV}\right)_B = k_B\left(\frac{dt}{dV}\right)_B^2 \tag{15}$$

Equation (15) describes the complete blocking process as proposed by Hermans and Bredee (7). Thus Eq. (12) as the description of the surface pore-blocking process is accepted as reasonable. Consequently, the filtration rate in the process controlled by both intrapore diffusion and surface blocking is given by

$$\left(\frac{dV}{dt}\right)_{D+B} = \left(\frac{dV}{dt}\right)_{D+B,0}\left(\frac{R_D}{R}\right)^4 \exp(-k_B t) \tag{16}$$

where the subscript $D+B$ means both intrapore diffusion and surface blocking controlling.

The blocking rate constant is distributed when various sizes of particles larger than the pore size are contained and the concentrations are distributed. Equation (16) has to be rewritten as

$$\left(\frac{dV}{dt}\right)_{D+B} = \left(\frac{dV}{dt}\right)_{D+B,0}\left(\frac{R_D}{R}\right)^4 \sum w_j \exp\left(-k_{B,j}t\right) \tag{17}$$

in the surface blocking process with discretely distributed rate constants, where $k_{B,j}$ is the jth component of the blocking rate constants and w_j is the spectrum density.

A thin cake layer is formed on the filter surface when the effective pore size becomes smaller than the particle size in the intrapore diffusion controlling period. The rate of filtration through the thin cake layer is described by Ruth's formula proposed for cake filtration, which is written as

$$\left(\frac{dV}{dt}\right)_c = \frac{1}{(2/K)V + (dt/dV)_{c,0}} \tag{18}$$

and hence,

$$\frac{d}{dV}\left(\frac{dt}{dV}\right)_c = \frac{2}{K} \tag{19}$$

is obtained, where the subscript c means cake formation controlling and K is Ruth's coefficient in constant pressure filtration.

NUMERICAL ANALYSIS

The filtration rate and the filtration resistance in the membrane microfiltration process dominated by diffusive deposition of particles on the inner walls of filter pores followed by cake formation were evaluated by numerical analysis. The variation of the filtration rate normalized by the initial rate, which will be called simply the filtration rate in the following description, with time is shown in Fig. 2 for various sizes of monodispersed particles. As can be seen, the larger the particle size, the shorter the diffusive deposition controlling period. The decrease of the filtration rate with time is suppressed after the cake layer is formed on the filter surface. The relationship between the filtration resistance normalized by the initial resistance and the increase of the filtration resistance per unit volume of the filtrate, which is normalized by the initial value, is shown in Fig. 3. These characteristics will be called simply the filtration resistance and the increase of the filtration resistance per unit volume of the filtrate, respectively, in the following description. The parallel

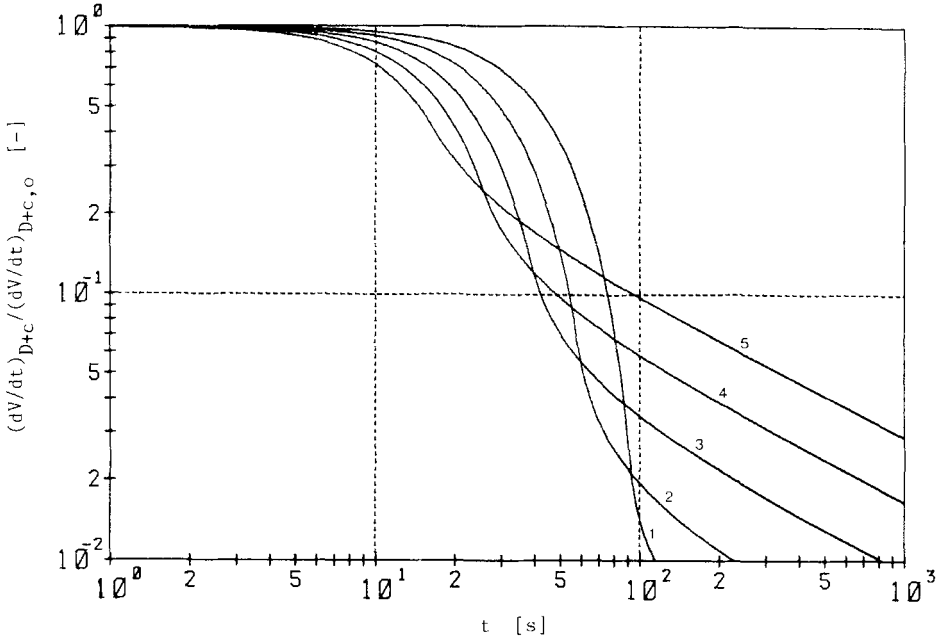

FIG. 2. Filtration rate for various sizes of monodispersed particles in the intrapore diffusive deposition and cake formation controlling process. $C_0 = 10^{13}$ m^{-3}. $R = 0.5$ μm. $L = 20$ μm. $k_D = 10^{-8}$ s^{-1}. $a = 0.20$ μm (1), 0.25 μm (2), 0.30 μm (3), 0.35 μm (4), 0.40 μm (5).

horizontal lines in the figure represent the characteristics in the cake formation period. It is found that the gradients of other linear parts connecting to the horizontal lines are about 2.4 for any particle sizes.

Other numerical calculations were carried out for microfiltration systems treating dilute suspensions containing various amounts of monodispersed particles. The filtration rates appear in Fig. 4. As can be seen, the higher the solids concentration, the shorter the intrapore deposition controlling period, and as a matter of course, the transition to cake filtration from intrapore filtration is observed at a fixed filtration rate. Moreover, each relationship between the filtration resistance and the increase of the filtration resistance per unit volume of the filtrate is illustrated in Fig. 5. Thus the gradients of the linear parts, except for the horizontal lines, are also found to be about 2.4.

The microfiltration characteristics were similarly analyzed for polydispersed systems. The effect of the particle sizes in the binary system on

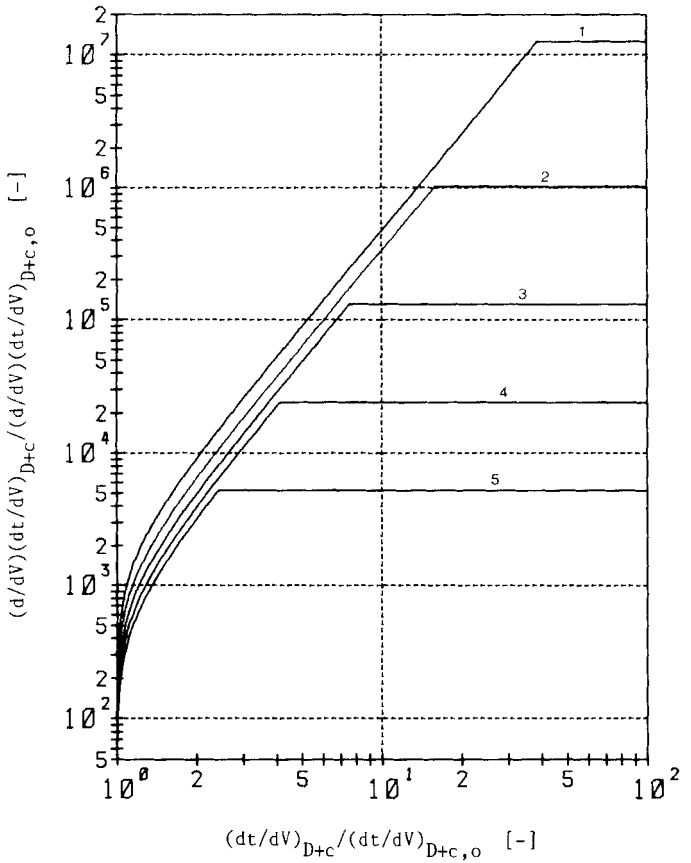

FIG. 3. Filtration resistance for various sizes of monodispersed particles in the intrapore diffusive deposition and cake formation controlling process. $C_0 = 10^{13}$ m^{-3}. $R = 0.5$ μm. $L = 20$ μm. $k_D = 10^{-8}$ s^{-1}. $a = 0.20$ μm (1), 0.25 μm (2), 0.30 μm (3), 0.35 μm (4), 0.40 μm (5).

the filtration rate is shown in Fig. 6. It is found that each pattern bears a resemblance to that illustrated in Fig. 2 or Fig. 4. The relationship between the filtration resistance and the increase of the filtration resistance per unit volume of the filtrate is shown in Fig. 7. As can be seen, the gradients of the linear parts are about 2.4, which is the same to the value obtained in the monodispersed system.

Furthermore, the filtration characteristics were evaluated in the microfiltration system with distributed deposition rate constants. The effects of the distribution of the rate constants on the filtration rate and

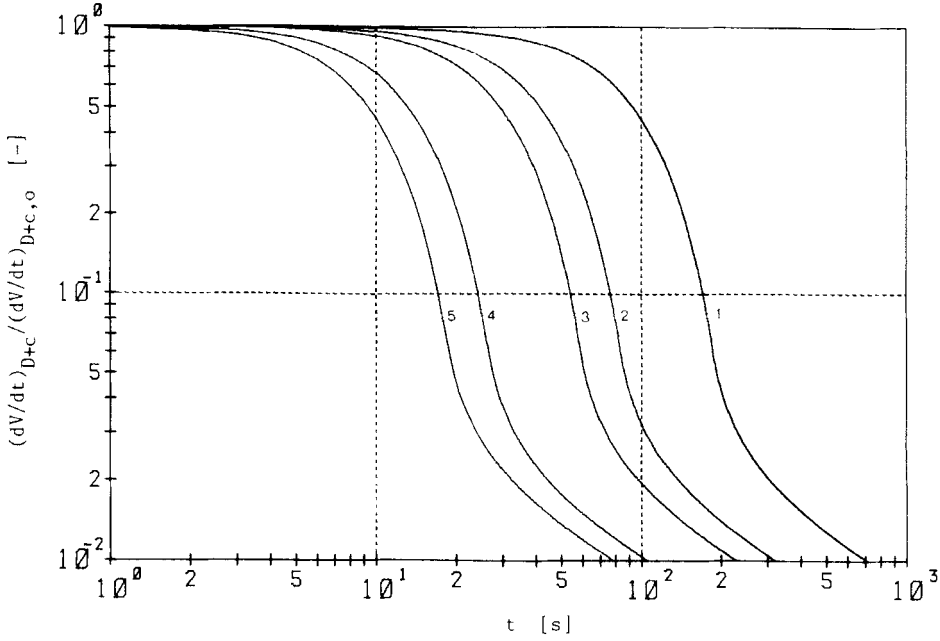

FIG. 4. Filtration rate for various concentrations of monodispersed particles in the intrapore diffusive deposition and cake formation controlling process. $a = 0.25$ μm. $R = 0.5$ μm. $L = 20$ μm. $k_D = 10^{-8}$ s^{-1}. $C_0 = 10^{12}$ m^{-3} (1), 5×10^{12} m^{-3} (2), 10^{13} m^{-3} (3), 5×10^{13} m^{-3} (4), 10^{14} m^{-3} (5).

the filtration resistance are illustrated in Figs. 8 and 9, respectively. The filtration characteristics are similar and are represented by parallel patterns. The gradients of the linear parts of the characteristic curves shown in Fig. 9 are also found to be about 2.4. Consequently, the filtration characteristics are formulated by

$$\frac{d}{dV}\left(\frac{dt}{dV}\right) = k\left(\frac{dt}{dV}\right)^n \tag{20}$$

in the intrapore diffusive deposition controlling period except for the initial stage, where the exponent n is about 2.4. Equation (20) is the same as the equation proposed by Hermans and Bredee (7). The simulation results obtained by using the macrokinetic models, however, give much larger values to the exponent n than those given by Hermans and Bredee. They proposed $n = 1$ for standard blocking and $n = 1.5$ for intermediate blocking.

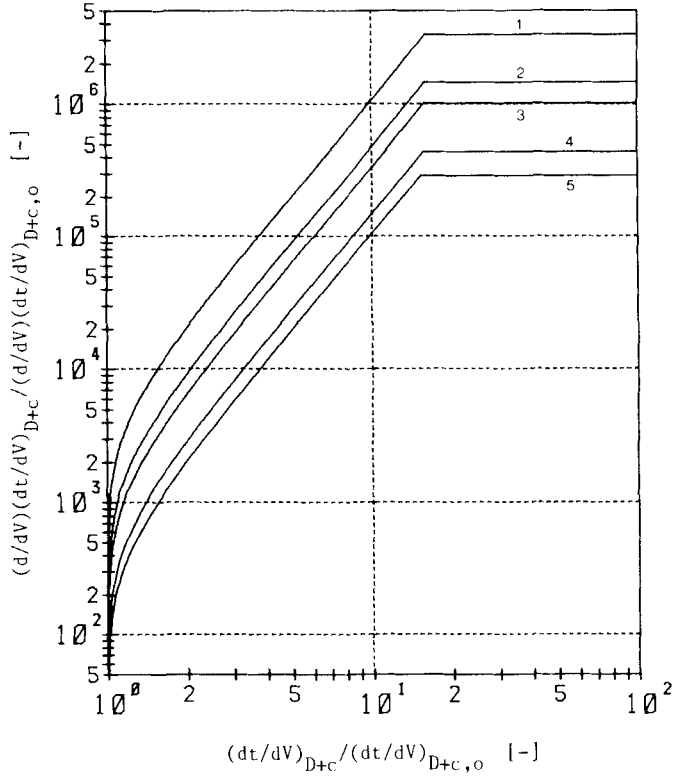

FIG. 5. Filtration resistance for various concentrations of monodispersed particles in the intrapore diffusive deposition and cake formation controlling process. $a = 0.25$ μm. $R = 0.5$ μm. $L = 20$ μm. $k_D = 10^{-8}$ s^{-1}. $C_0 = 10^{12}$ m^{-3} (1), 5×10^{12} m^{-3} (2), 10^{13} m^{-3} (3), 5×10^{13} m^{-3} (4), 10^{14} m^{-3} (5).

Then the membrane microfiltration process dominated by both intrapore diffusive deposition and surface pore blocking was numerically analyzed. The relationship between the filtration resistance and the increase of the filtration resistance per unit volume of the filtrate is shown in Fig. 10 where the blocking rate constant is varied. The relationship in the distributed blocking rate constants system is shown in Fig. 11. As can be seen from Fig. 10, the filtration characteristics are also formulated by Eq. (20) except for the initial filtration period, and the larger the blocking rate constant, the smaller the exponent n. Thus the exponent n varies between about 2.4 for intrapore diffusive deposition controlling and 2 for surface pore blocking controlling. It is, however, observed in Fig. 11 that

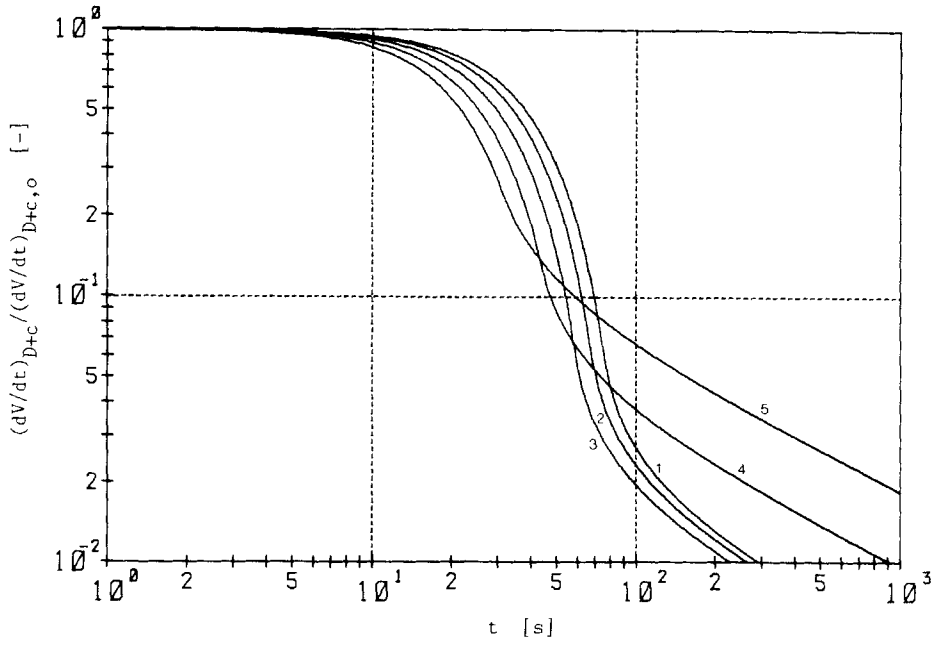

FIG. 6. Filtration rate for various sizes of binary dispersed particles in the intrapore diffusive deposition and cake formation controlling process. $a_2 = 0.25$ μm. $R = 0.5$ μm. $L = 20$ μm. $C_{0,1} = C_{0,2} = 5 \times 10^{12}$ m^{-3}. $k_{D,1} = k_{D,2} = 10^{-8}$ s^{-1}. $a_1 = 0.15$ μm (1), 0.20 μm (2), 0.25 μm (3), 0.30 μm (4), 0.35 μm (5).

Eq. (20) cannot be applied to characterize the filtration performance in the distributed blocking rate constants system. Thus the membrane microfiltration behaviors in this system are complicated, and they depend on the magnitude of the distributed rate constants and the spectrum densities.

VERIFICATION OF THE MACROKINETIC MODELS

The macrokinetic models for membrane microfiltration were verified through a series of filtration tests carried out under constant pressure. The filter media used in the experiments were Nuclepore filter (Nomura Micro Science) and Millipore filter (Japan Millipore). Their nominal pore diameters were 0.6 and 0.45 μm, respectively. The Nuclepore filter is made of polycarbonate and the pore configuration is cylindrical. The materials used were α-alumina particles which were chemically synthe-

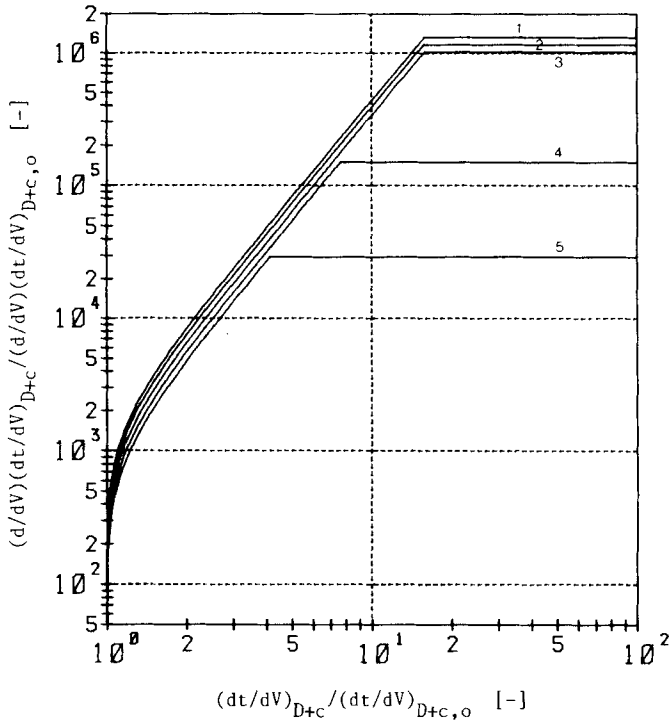

FIG. 7. Filtration resistance for various sizes of binary dispersed particles in the intrapore diffusive deposition and cake formation controlling process. $a_2 = 0.25$ μm. $R = 0.5$ μm. $L = 20$ μm. $C_{0.1} = C_{0.2} = 5 \times 10^{12}$ m^{-3}. $k_{D.1} = k_{D.2} = 10^{-8}$ s^{-1}. $a_1 = 0.15$ μm (1), 0.20 μm (2), 0.25 μm (3), 0.30 μm (4), 0.35 μm (5).

sized to involve in a few size classes. The particles involved in a single size class or the particles prepared by mixing of particles involved in two size classes were suspended in deionized water filtered by a 0.1 μm Millipore filter to obtain a predetermined solids concentration and then the particles were dispersed in the stirred supersonic bath for 1 h. Operating pressure was regulated by a control valve and a pressure sensor and held at 2×10^4 Pa. The solids concentration in the filtrate was detected by a calibrated turbidity meter, while the flow rate of the filtrate was measured by using the load cell. Signals from these instruments were acquired in the microcomputer system through a A/D converter in which sampled signals were smoothed, and the filtration characteristics were calculated.

The relationship between the filtration resistance and the increase of

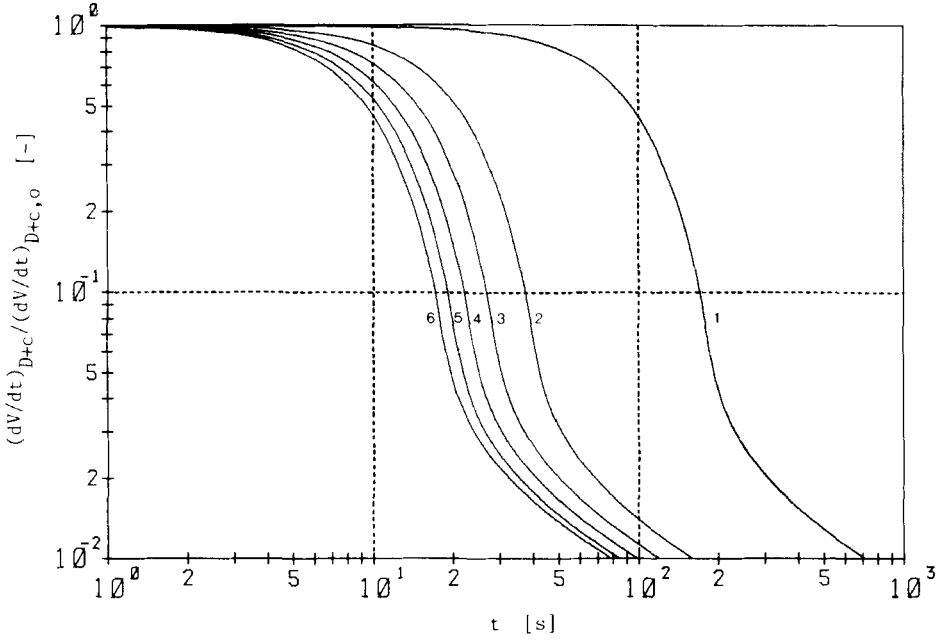

FIG. 8. Filtration rate for monodispersed particles in the intrapore diffusive deposition and cake formation controlling process with distributed deposition rate constants. $C_0 = 10^{13}$ m^{-3}. $a = 0.25$ μm. $R = 0.5$ μm. $L = 20$ μm. $k_{D,1} = 10^{-9}$ s^{-1}. $k_{D,2} = 10^{-7}$ s^{-1}. (1): $w_1 = 1$, $w_2 = 0$. (2): $w_1 = 0.8$, $w_2 = 0.2$. (3): $w_1 = 0.6$, $w_2 = 0.4$. (4): $w_1 = 0.4$, $w_2 = 0.6$. (5): $w_1 = 0.2$, $w_2 = 0.8$. (6): $w_1 = 0$, $w_2 = 1$.

the filtration resistance per unit volume of the filtrate was first observed in the system controlled by intrapore diffusive deposition of particles. Some of the results are shown in Fig. 12. As can be seen, Eq. (20) is realized except for the cake formation period, and the exponent n is confirmed to be about 2.4 for any solids concentration as predicted by the macrokinetic model. Moreover, the formation of the thin cake layer characterized by Eq. (19) is observed in the final stage of filtration.

Similar filtration characteristics observed by using mixed particles composed of various amounts of smaller and larger particles than the filter pore size are shown in Fig. 13. It is also confirmed that Eq. (20) is realized except for the final stage of filtration, and the exponent n becomes smaller as the concentration of particles larger than the pore size is increased. Thus the transition of filtration behavior to surface blocking controlling from intrapore diffusive deposition controlling is

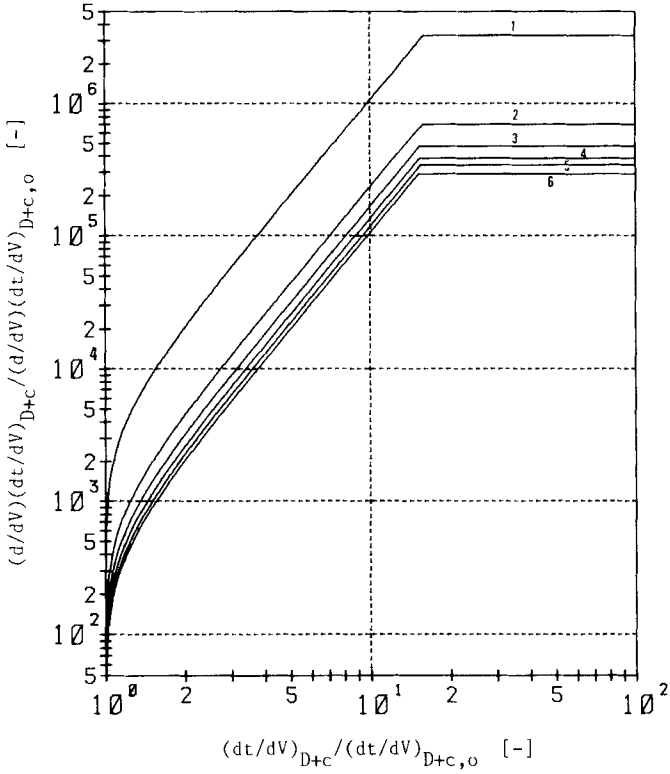

FIG. 9. Filtration resistance for monodispersed particles in the intrapore diffusive deposition and cake formation controlling process with distributed deposition rate constants. $C_0 = 10^{13}$ m^{-3}. $a = 0.25$ μm. $R = 0.5$ μm. $L = 20$ μm. $k_{D,1} = 10^{-9}$ s^{-1}. $k_{D,2} = 10^{-7}$ s^{-1}. (1): $w_1 = 1$, $w_2 = 0$. (2): $w_1 = 0.8$, $w_2 = 0.2$. (3): $w_1 = 0.6$, $w_2 = 0.4$. (4): $w_1 = 0.4$, $w_2 = 0.6$. (5): $w_1 = 0.2$, $w_2 = 0.8$. (6): $w_1 = 0$, $w_2 = 1$.

confirmed experimentally with the increase of the concentration of particles larger than the filter pore size.

Although the pore structure of the Millipore filter is complicated and differs from that supposed in deriving the macrokinetic models, the simulation results agree well with the experimental observations. Consequently, the proposed macrokinetic models has been successfully verified and hence the models will be useful tools to analyze, predict, and optimize the filtration processes if each kinetic rate constant can be easily correctly evaluated.

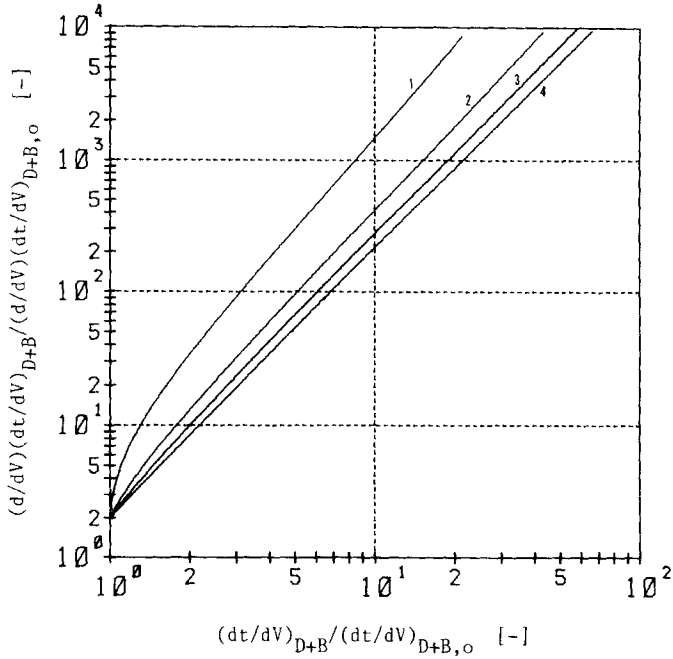

FIG. 10. Filtration resistance in the intrapore diffusive deposition and pore blocking controlling process. $C_0 = 10^{13}$ m^{-3}. $a = 0.25$ μm. $R = 0.5$ μm. $L = 20$ μm. $k_D = 10^{-8}$ s^{-1}. $k_B = 0.01$ s^{-1} (1), 0.03 s^{-1} (2), 0.05 s^{-1} (3), 0.10 s^{-1} (4).

FURTHER DEVELOPMENT OF THE KINETIC APPROACH

It is important in practical operation to incorporate the backflushing stage in the main microfiltration system. The detachment process for collected fine particles from a packed bed composed of coarse particles by backwashing was investigated experimentally because the detachment characteristics were considered to be analogous to those of diffusively deposited particles in the backflushing stage of membrane microfiltration. As a result, the detachment process was regarded macroscopically as a first-order rate process with a fixed rate constant or a few distributed rate constants. It is believed that the detachment process of monodispersed particles at the backflushing stage of membrane microfiltration is described basically by

$$-dC_D/dt = k_F C_D \tag{21}$$

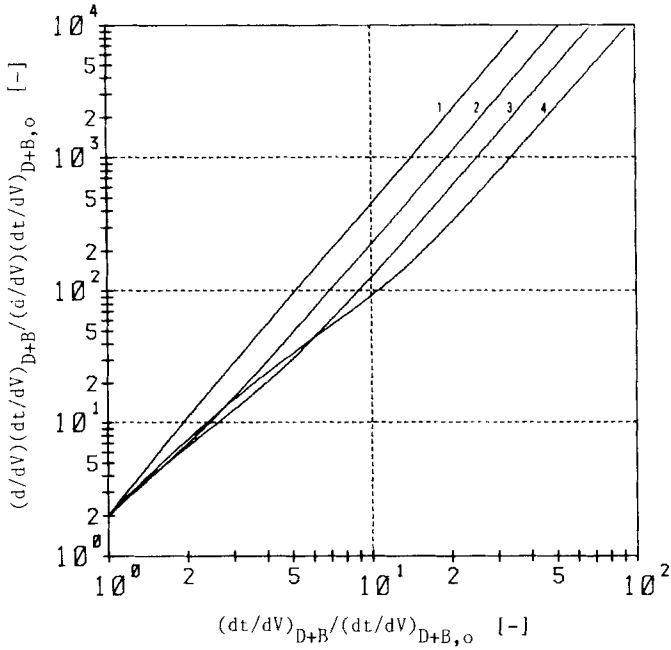

FIG. 11. Filtration resistance in the intrapore diffusive deposition and pore blocking controlling process with distributed blocking rate constants. $C_0 = 10^{13}$ m^{-3}. $a = 0.25$ μm. $R = 0.5$ μm. $L = 20$ μm. $k_D = 10^{-8}$ s^{-1}. $k_{B,1} = 0.01$ s^{-1}. $k_{B,2} = 0.10$ s^{-1}. (1): $w_1 = 0.8$, $w_2 = 0.2$. (2): $w_1 = 0.6$, $w_2 = 0.4$. (3): $w_1 = 0.4$, $w_2 = 0.6$. (4): $w_1 = 0.2$, $w_2 = 0.8$.

where C_D is the concentration of diffusively deposited particles and k_F is the detachment rate constant in the backflushing stage. Hence,

$$C_D = C_{D,0} \exp(-k_F t) \tag{22}$$

is obtained, where $C_{D,0}$ is the initial concentration of deposited particles. Equation (22) is rewritten as

$$C_D = C_{D,0} \sum w_j \exp(-k_{F,j} t) \tag{23}$$

when the detachment rate constant is distributed discretely, where $k_{F,j}$ is the jth component of the detachment rate constants, and w_j is the spectrum density.

The filtration characteristics of a membrane microfiltration system involving backflushing stages can be evaluated by using Eqs. (6) and (22)

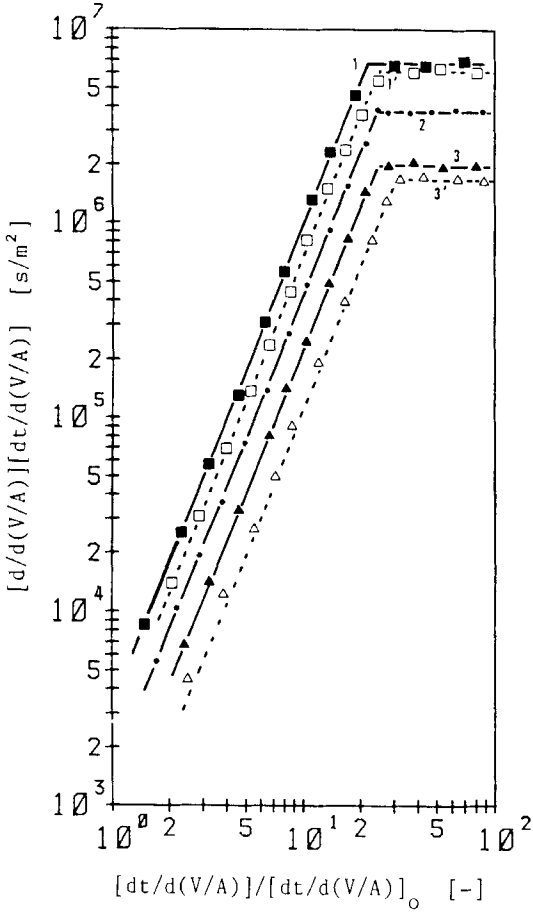

FIG. 12. Experimental observations on the filtration resistance for pseudomonodispersed particles in the intrapore diffusive deposition and cake formation controlling processes. (1, 2, 3): Nucleopore filter. (1′, 3′): Millipore filter. (1, 1′): C_0 = 8 ppm. (2): C_0 = 4 ppm. (3, 3′): C_0 = 1 ppm.

if there is only intrapore diffusive deposition controlling. The effect of backflushing on the filtration rate of monodispersed particles is shown in Fig. 14, where the total operating time is constant and the ratio of the backflushing time (t_F) to the filtration time (t_D) is varied. The abscissa in this figure is the integration of the filtration time. How to determine the filtration time and the backflushing time is one of the most important problems in a practical microfiltration process. These operating parame-

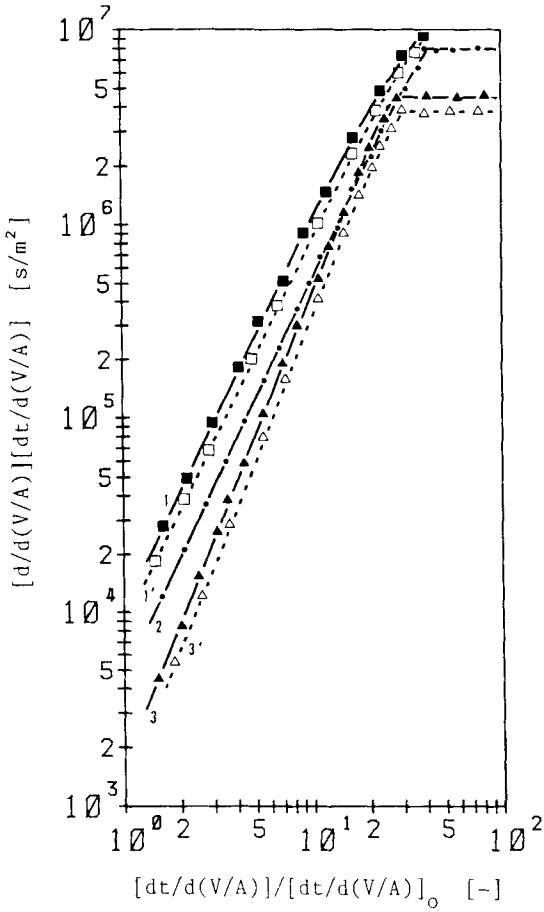

FIG. 13. Experimental observations on the filtration resistance in the intrapore diffusive deposition and pore blocking controlling processes. (1, 2, 3): Nuclepore filter. (1', 3'): Millipore filter. (1, 1'): $C_0(a > R) = 2$ ppm, $C_0(a < R) = 2$ ppm. (2): $C_0(a > R) = 1$ ppm, $C_0(a < R) = 3$ ppm. (3, 3'): $C_0(a > R) = 0.1$ ppm, $C_0(a < R) = 4$ ppm.

ters have hitherto been determined empirically. However it must be possible to determine the most effective conditions and to predict the filtration performance by applying the extended macrokinetic model to a practical filtration process.

The extended model was also applied to the polydispersed system. The effect of backflushing on the filtration rate of polydispersed particles is shown in Fig. 15, where each concentration of particles involved in four

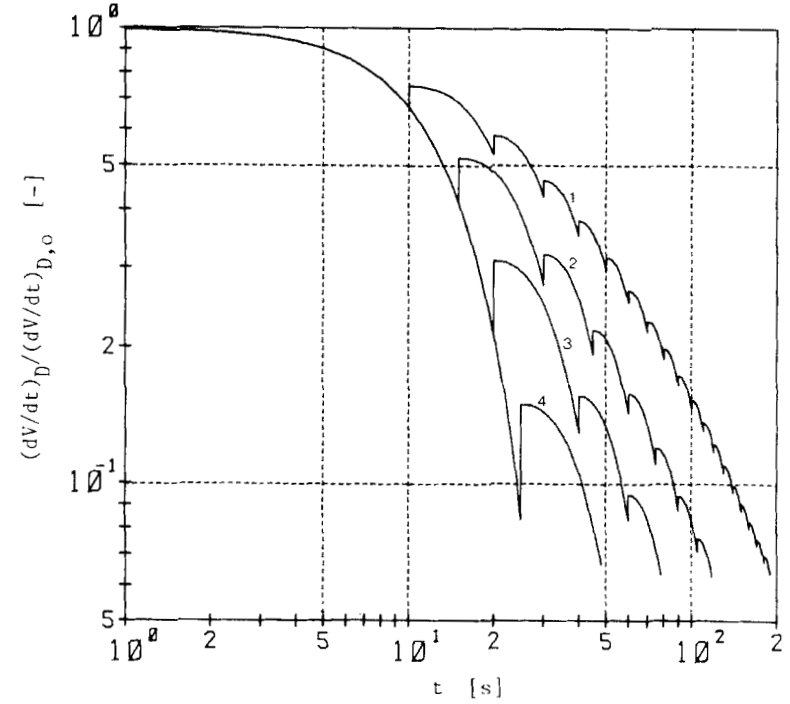

FIG. 14. Effect of backflushing on the filtration rate for monodispersed particles. $C_0 = 5 \times 10^{13}$ m^{-3}. $a = 0.25$ μm. $R = 0.5$ μm. $L = 20$ μm. $k_D = 10^{-8}$ s^{-1}. $k_F = 0.01$ s^{-1}. (1): $t_D = 10$ s, $t_F = 30$ s. (2): $t_D = 15$ s, $t_F = 25$ s. (3): $t_D = 20$ s, $t_F = 20$ s. (4): $t_D = 25$ s, $t_F = 15$ s.

size classes is varied while keeping the total concentration constant, the filtration time, the backflushing time, the deposition rate constant, and the backflushing rate constant are kept constant. As can be seen, the filtration performance is significantly affected by the size distribution of particles. The detachment rate of particles depends on their size and the filter pore configuration. The deposition rate constant or the detachment rate constant has to be evaluated as a function of the particle size distribution to draw a precise picture of the microfiltration behavior in the polydispersed system. As an example, the effect of a variation of the backflushing rate constant with particle size on the filtration rate is shown in Fig. 16. The filtration performance is more improved when the backflushing rate constant is increased with particle size. The variation of the backflushing rate constant with particle size depends on the structure of the filter medium and the physical as well as the chemical properties of the particles.

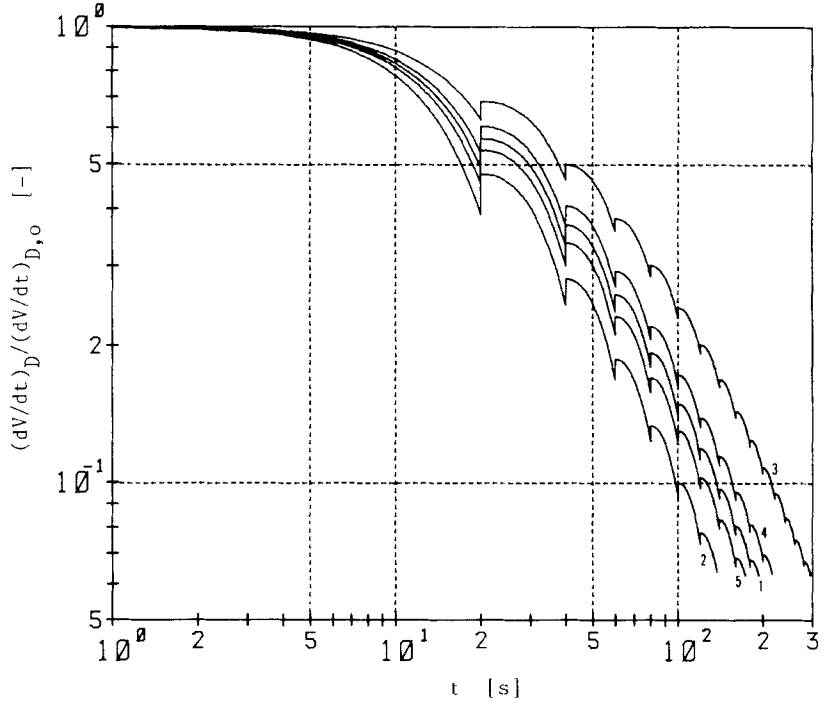

FIG. 15. Effect of backflushing on the filtration rate for polydispersed particles. R = 0.5 μm. L = 20 μm. $k_D = 10^{-8}$ s^{-1}. k_F = 0.01 s^{-1}. t_D = 20 s. t_F = 20 s. $C_{0,i}$[× 10^{13} m^{-3}]:

a_i [μm]	1	2	3	4	5
0.10	1.25	0.50	2.00	0.50	2.00
0.15	1.25	1.00	1.50	2.00	0.50
0.20	1.25	1.50	1.00	2.00	0.50
0.25	1.25	2.00	0.50	0.50	2.00

CONCLUSION

The membrane microfiltration process for a solid-liquid system is characterized by the intrapore diffusive deposition of finer particles on the inner walls of the filter pores, the surface pore blocking by larger particles than the pore size, and the formation of a thin cake layer on the filter surface. The diffusive deposition process is analyzed by a diffusion equation describing the particle behavior in a filter pore, and it is regarded as a first-order rate process. The filtration characteristics are

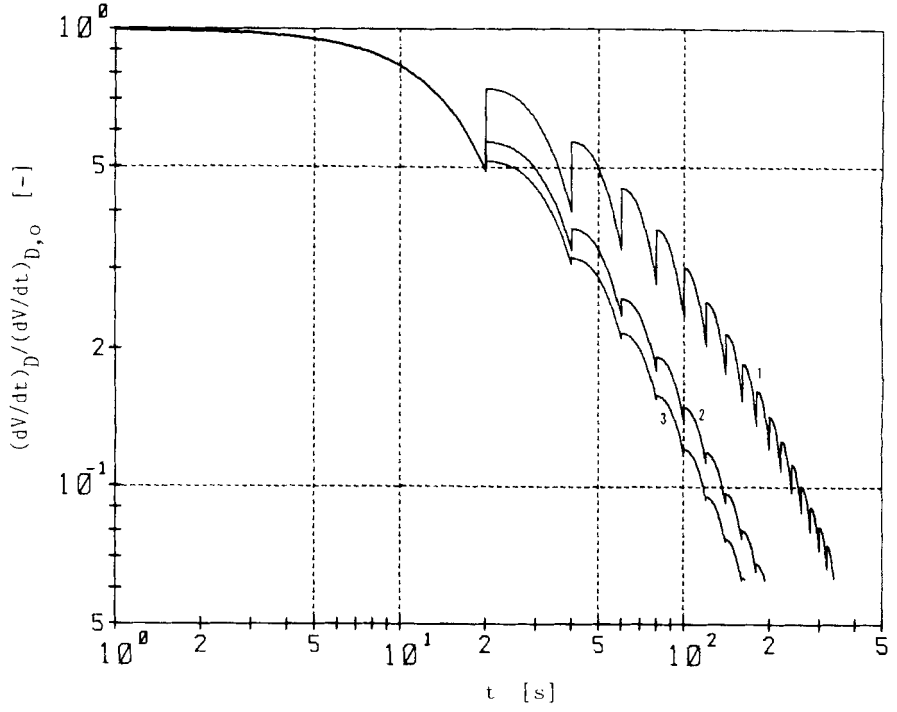

FIG. 16. Effect of backflushing on the filtration rate for polydispersed particles with detachment rate constants varied with particle sizes. $R = 0.5$ μm. $L = 20$ μm. $C_{0,1} = C_{0,2} = C_{0,3} = C_{0,4} = 1.25 \times 10^{13}$ m^{-3}. $k_{D,1} = k_{D,2} = k_{D,3} = k_{D,4} = 10^{-8}$ s^{-1}. k_F[s^{-1}]:

a_i [μm]	1	2	3
0.10	10^{-4}	10^{-2}	10^{-1}
0.15	10^{-3}	10^{-2}	10^{-2}
0.20	10^{-2}	10^{-2}	10^{-3}
0.25	10^{-1}	10^{-2}	10^{-4}

numerically analyzed for not only a monodispersed system but also for a polydispersed and distributed rate constants system by using the macrokinetic models derived from first-order rate equations. Thus the relationship between the filtration resistance and the increase of the filtration resistance per unit volume of the filtrate is represented by a simple power law (Eq. 20) except for the initial and cake formation stages, the exponent of which is about 2.4 under any operating conditions. These macrokinetic models are verified through a series of filtration tests.

The surface pore blocking process is also described by a first-order rate equation. A macrokinetic model is proposed to evaluate the filtration characteristics in the microfiltration system controlled by both intrapore diffusive deposition and surface pore blocking. Equation (20) is realized in any systems with fixed blocking rate constants, and the exponent varies between about 2.4 for intrapore diffusive deposition controlling and 2 for surface pore blocking controlling. The filtration characteristics are, however, more complicated when the blocking rate constant is distributed, and they cannot be represented by Eq. (20). The theoretical results agree well with experimental observations.

Backflushing is essential to improve filtration performance in practical operation. The detachment process of collected particles from filter pores is regarded as a first-order rate process, and the macrokinetic model is extended to simulate the microfiltration system with backflushing stages. The filtration characteristics are evaluated in terms of the detachment rate constant and the backflushing time by using the extended macrokinetic model.

Consequently, the proposed macrokinetic models will be useful tools to analyze, predict, and optimize the microfiltration processes if each kinetic parameters can be easily evaluated correctly.

SYMBOLS

A	filter area (m^2)
a	particle radius (m)
C	solids concentration on count basis ($1/m^3$)
C_D	concentration of diffusively deposited particles ($1/m^3$)
C_0	initial solids concentration ($1/m^3$)
D	diffusion coefficient (m^2/s)
K	Ruth's coefficient in constant pressure filtration (m^6/s)
k	constant involved in Eq. (20)
k_B	blocking rate constant (1/s)
k_D	diffusive deposition rate constant (1/s)
k_F	detachment rate constant (1/s)
L	pore length (m)
M	number of unblocked pores per unit filter area ($1/m^2$)
M_0	number of pores per unit filter area ($1/m^2$)
N	dimensionless concentration involved in Eq. (2)
n	constant involved in Eq. (20)
Pe	Peclet number
R	pore radius (m)

r	radial coordinate
R_D	effective pore radius (m)
t	time (s)
t_D	filtration time (s)
t_F	backflushing time (s)
U	dimensionless velocity involved in Eq. (2)
u_0	axial flow velocity at $r = 0$ (m/s)
u_z	axial flow velocity (m/s)
V	flow volume (m^3)
w	spectrum density of the rate constant
x, y	dimensionless coordinates involved in Eq. (2)
z	axial coordinate

Greek

$\delta(t)$	Dirac's delta function
θ	mean residence time (s)
τ	dimensionless time involved in Eq. (2)

Subscripts

B	surface pore blocking
c	cake formation
D	intrapore diffusive deposition
$D+B$	diffusive deposition and blocking
$D+c$	diffusive deposition and cake formation
i	component of particle sizes
j	component of spectrum densities
0	initial state

Acknowledgments

The author wishes to thank Sumitomo Chemical Industry Corp. Ltd. for the preparation of the materials and Mr S. Matsuo, technical assistant of the Department of Mineral Development Engineering, The University of Tokyo, for his great efforts on the laborious experimental work.

REFERENCES

1. J. Pich, *Collect. Czech. Chem. Commun., 29,* 2223 (1964).
2. K. Spurny and J. P. Lodge, *Ibid., 33,* 3679 (1968).

3. K. Spurny and J. P. Lodge, *Staub, 28,* 179 (1968).
4. T. N. Smith, C. R. Phillips, and O. T. Melo, *Environ. Sci. Technol., 9,* 564 (1975).
5. R. D. Parker and G. H. Buzzard, *J. Aerosol Sci., 9,* 7 (1978).
6. B. F. Towler and R. Y. K. Yang, *Chem. Eng. J., 12,* 81 (1976).
7. P. H. Hermans and H. L. Bredee, *J. Soc. Chem. Ind., 55,* 1T (1936).

Received by editor May 18, 1987